

Reactions between  $^{20}\text{Ne}$  and nickel

Felix E. Obenshain, R. L. Ferguson, M. L. Halbert, D. C. Hensley, H. Nakahara,\* F. Plasil, F. Pleasonton, A. H. Snell, and R. G. Stokstad

Oak Ridge National Laboratory,<sup>†</sup> Oak Ridge, Tennessee 37830

(Received 13 February 1978)

Charge, energy, and angular distributions of products from reactions between  $^{20}\text{Ne}$  and Ni have been measured at 164 MeV. The total reaction cross section inferred from the quarter-point of the elastic scattering data is 2010 mb. Products with  $6 \leq Z \leq 20$  account for 30% of the total reaction cross section. The evaporation residue cross section was also measured and found to be 1236 mb, or 61% of the total cross section. Products with atomic number near that of the projectile have angular distributions which increase in the forward direction and have energy spectra characteristic of both quasielastic and deeply inelastic events. Products with atomic numbers greater than 14 show an angular distribution  $d\sigma/d\Omega \propto 1/\sin\theta_{\text{c.m.}}$  and have kinetic energies that are characteristic of Coulomb repulsion following binary fission, indicating that complete damping has occurred. However, the yield near  $Z = 19$  is low, and thus symmetric fission, if present at all, accounts for a rather small fraction of the total reaction cross section.

NUCLEAR REACTIONS  $^{20}\text{Ne} + \text{Ni}$ ;  $E = 164$  MeV; strongly damped;  $10^\circ \leq \psi_{\text{lab}} \leq 70^\circ$ ; quasielastic; product energies, charge distributions, cross sections  $d\sigma/d\theta_{\text{c.m.}}$ ; evaporation residue cross section  $\sigma_{\text{ER}}$ ; reaction cross section; gas ionization detector  $\Delta E$ ; surface barrier detector  $E$ .

## I. INTRODUCTION

Deeply inelastic collisions between heavy ions and target nuclei have been the subject of considerable interest since their original investigation by Artukh *et al.*<sup>1</sup> This interest has been intensified by the observation that for very heavy systems, deeply inelastic collisions account for a very large fraction of the total reaction cross section.<sup>2,3</sup> The main feature of these reactions is the considerable damping of the energy of the incoming projectile, which may be accompanied by a relatively large transfer of mass and charge. While a large number of systems involving very heavy ions ( $A \approx 40$ ) and heavy targets ( $A \approx 100$ ) have been investigated and interpreted in terms of a variety of theoretical models,<sup>4</sup> only a few studies have been made with lighter ions incident on relatively light nuclei.<sup>5-16</sup> The region of composite system mass numbers ranging from about 60 to 120 is of particular interest to us, since it involves nuclei that are fairly light, but also sufficiently heavy so that nuclear structure and single-particle effects are not expected to dominate the reactions.

In undertaking this work, we have been governed by two main motivations: First, we wished to establish the features of the deep inelastic reactions in this region of nuclei and compare them with the well-established features of these reactions in the heavier systems. Second, we wished

to see to what extent, if any, fission takes place in these relatively light systems, and what its characteristics are.<sup>17</sup> In this paper we present results from  $^{20}\text{Ne}$  bombardments of nickel at 164 MeV. Preliminary results for the same reaction, but primarily at 173 MeV, were reported earlier.<sup>18</sup> In addition, some results for related systems  $^{20}\text{Ne} + ^{48}\text{Ti}$  and  $^{20}\text{Ne} + ^{94}\text{Zr}$  have been presented.<sup>19</sup>

Previous work involving composite systems with  $50 < A < 100$  includes  $^{16}\text{O} + \text{Ni}$  at 96 MeV,<sup>6</sup>  $^{40}\text{Ar} + ^{58}\text{Ni}$  at 280 MeV,<sup>7</sup>  $^{32}\text{S} + ^{50}\text{Ti}$  at 105 to 166 MeV,<sup>8-11</sup> and  $^{35}\text{Cl} + ^{27}\text{Al}$  at 140 to 170 MeV.<sup>12,13</sup> Thus our system involves a relatively higher relative velocity (higher MeV per nucleon) and a lighter projectile (with the exception of Ref. 6) than have been studied previously. The existence of deeply inelastic reactions in this region has been established in Refs. 6 and 7 and confirmed in later work. In Refs. 9 and 12 the binary nature of these processes was established by means of coincidence experiments, and the question of fission was specifically addressed for the systems  $^{32}\text{S} + ^{50}\text{Ti}$  and  $^{35}\text{Cl} + ^{27}\text{Al}$  in Refs. 10-12. It was observed that yields of fissionlike products were obtained and that their properties followed fission systematics. Certain ambiguities as to the nature of these products, however, remained.

Models involving transport theory, energy dissipation, angular momentum transfer and other fundamental bulk properties of nuclei are being

successfully applied to deeply inelastic reactions in heavier systems.<sup>4</sup> It is our intent, once sufficient systematic data are available, to test the range of validity of some of these models by applying them in this relatively light region. As far as fission is concerned, as was pointed out above, the situation remains ambiguous.<sup>10-12, 17</sup> The large angular momenta involved in heavy ion reactions are expected to lower the fission barrier of rotating compound nuclei sufficiently to make fission a competing deexcitation process,<sup>20-22</sup> and, indeed, fissionlike events have been observed. It is, however, difficult to distinguish fission from those deeply inelastic processes that involve both a large amount of mass transfer and an interaction time of the order of several rotations, resulting in an angular distribution that is uniform in  $d\sigma/d\theta$  in the center-of-mass system. It is possible that the near-zero fission barrier inhibits the formation of compound nuclei in the first place, and it is difficult to confirm the presence of fission experimentally due to a lack of a specific signature of the process in this light region.

In Sec. II we describe the experimental method, and in Sec. III we present the results. In Sec. III the total reaction cross section is considered first, and the component cross sections are discussed in order of decreasing impact parameter  $b$ . The quasielastic, deeply inelastic collisions and fission and evaporation residue products are described.

## II. APPARATUS AND EXPERIMENTAL PROCEDURE

Experiments were done at the Oak Ridge Isochronous Cyclotron (ORIC) with beams of  $^{20}\text{Ne}^{6+}$  heavy ions at two different energies, 164 and 173 MeV. Results obtained at the two energies were very similar to each other, and only data obtained at 164 MeV will be presented here; the 173 MeV results are given in Ref. 18.

The targets were self-supporting natural nickel foils. Data from two foils, one 113 and the other 704  $\mu\text{g}/\text{cm}^2$ , were compared and no significant difference in the relative charge yields was noted. Since the increased yield from the thicker target served to decrease counting times, the major part of the results were obtained with it. Typical beam currents were 20 electrical nA.

The data were taken with two different charged-particle detector systems. Each consisted of a gas ionization chamber to obtain the energy loss  $\Delta E$ , and a silicon surface-barrier detector to

record the remaining energy ( $E - \Delta E$ ). One system consisted of a multiangle telescope with a position-sensitive silicon detector,<sup>23</sup> and the other was a small-aperture single-angle telescope with a 25 mm<sup>2</sup> silicon detector. The latter telescope was necessary to measure products in the forward direction. The entrance windows were Formvar films about 50  $\mu\text{g}/\text{cm}^2$  thick. The methane gas pressure was 48 Torr (corresponding to 361  $\mu\text{g}/\text{cm}^2$ ).

The multiangle telescope provided nine spectra at 1° intervals for each angular setting. The  $(\Delta E, E')$  data were recorded in nine two-parameter arrays. The energy  $E'$  was obtained by analog addition of  $\Delta E$  to  $(E - \Delta E)$ . An energy spectrum for each nuclear charge  $Z$  was obtained from the arrays by the appropriate masking of the  $(\Delta E, E')$  contour maps. The first and last intervals of the position-sensitive detector showed a large decrease in detection efficiency for smaller values of nuclear charge than the projectile and in particular in the forward direction. This was attributed to end effects and the data were discarded.

The data were converted from laboratory to center-of-mass coordinates with the assumption of two-body kinematics.<sup>9, 12</sup> The mass  $A_c$  for the composite system is 78, and for the light fragment  $A_1$  the mass is taken as  $2Z$ , where  $Z$  is the observed nuclear charge. The mass of the heavy fragment was assumed to be  $A_2 = A_c - A_1$ . Since the observed charge  $Z$  is after particle evaporation, the above procedure leads to some errors in the center-of-mass distributions. This problem of particle evaporation is treated in some detail in Sec. III C, but here its effect on the center-of-mass transformations is considered negligible. In order to obtain a continuous distribution in the energy-angle coordinates, an interpolation procedure was used to obtain intermediate energies and angles. Grid fluctuations introduced by the transformation due to finite angle and energy resolution were minimized by adding appropriately scaled random numbers during the transformation process.

The effect of target impurities was investigated by bombarding carbon targets with Ne ions and by comparing the distributions obtained with the Ni data. We are able to conclude that Ne reactions with target contaminants, such as carbon and oxygen, if any, do not contribute an observable amount to our cross sections.

Data from our various angles were normalized by means of fixed monitor detectors, and absolute cross sections were obtained by normalizing to elastic scattering at small angles where the scattering is assumed to be Rutherford.

### III. RESULTS AND DISCUSSION

The total reaction cross section, deduced from elastic scattering data, is discussed in Sec. III A. This cross section can be divided into a quasi-elastic (QE) contribution, a deeply inelastic contribution (DI), and an evaporation residue (ER) part, discussed in Secs. III B, III C, and III D, respectively. Fission is considered together with deeply inelastic reactions in Sec. III C.

#### A. Total reaction cross section

The total reaction cross section may be determined from measurements of the elastic scattering at forward angles following the  $\frac{1}{4}$ -point method of Blair.<sup>24</sup> The elastic cross section was found to decrease to one-fourth of Rutherford at  $(17.7 \pm 0.5)^\circ$  in the laboratory system or  $23.7^\circ$  in the center-of-mass system (c.m.). The total reaction cross section for heavy ions is given by a sum of partial cross sections for definite orbital angular momenta weighted by the barrier transmission probabilities

$$\sigma_R = \pi \lambda^2 \sum_{l=0}^{\infty} (2l+1) T_l. \quad (1)$$

In the sharp cutoff approximation, the transmission coefficients  $T_l$  are put equal to unity for  $l \leq l_{\max}$  and zero for  $l > l_{\max}$ . Thus the summation over  $l$  yields

$$\sigma_R = \pi \lambda^2 (l_{\max} + 1)^2. \quad (2)$$

The de Broglie wavelength  $\lambda$  is  $1.07 \times 10^{-14}$  cm, and a value for the angular momentum quantum number  $l_{\max}$  is calculated from the expression

$$l_{\max} = \eta \cot\left(\frac{1}{2} \theta_{\text{c.m.}}\right), \quad (3)$$

where  $\theta_{\text{c.m.}}$  is the center-of-mass scattering angle and  $\eta$  is the Sommerfeld parameter. The value of  $l_{\max} \cong 73$  is obtained with  $\eta = 15.4$  and  $\theta_{\text{c.m.}} = 23.7^\circ$ . The total reaction cross section calculated by this method is  $2010 \pm 80$  mb.

As was discussed above, the total reaction cross section  $\sigma_R$  may be thought to consist of a quasi-elastic component, a deeply inelastic component and a fusion contribution. Anticipating our results for these other processes, we may check whether the above value of  $\sigma_R$  does in fact agree with the sum of the others. While our results indicate the existence of distinct QE and DI processes, it is hazardous to decompose them quantitatively, and we have not attempted to do so. The measured evaporation-residue cross section has to be combined with fission to obtain the fusion

cross section. We are unable to identify a separate fission component; its contribution, if any, is included in the DI component. Thus we compare  $\sigma_R$  with  $\sigma_{\text{IN}} + \sigma_{\text{ER}}$ , where  $\sigma_{\text{IN}}$  denotes the sum of QE, DI, and fission processes and where  $\sigma_{\text{ER}}$  is the evaporation-residue cross section. The experimental cross section  $\sigma_{\text{IN}}$  was found to be  $625 \pm 25$  mb and  $\sigma_{\text{ER}} = 1236 \pm 50$  mb (see Sec. III D). Their sum,  $1861 \pm 75$  mb, compares favorably with  $\sigma_R$  of  $2010 \pm 80$  mb deduced above.

#### B. Quasielastic reactions

A quasielastic component for products with charges near the projectile ( $Z = 10$ ) is observed, as can be seen in the energy spectra of Figs. 1–3 at  $\theta_{\text{c.m.}} = 17^\circ, 24^\circ,$  and  $35^\circ$ , respectively. These events are represented by the peaks in the spectra at the highest energies and correspond to velocities nearly equal to the primary beam of  $^{20}\text{Ne}$ . In some cases (charges 9, 10, and 11) the quasi-elastic events could be resolved from the strongly damped events, but in general there is a continuous distribution of events from the quasi-elastic region to the deeply inelastic region. The angular distributions associated with the quasi-elastic events are forward peaked and their cross section becomes negligible some  $10^\circ$  beyond the grazing angle. This is in accord with the expectation that they are principally few nucleon transfer reactions, which are known to decrease strongly beyond the grazing angle.

The energy of the incident neon is 8.2 MeV/nucleon in the laboratory system and the quasi-elastic events should differ in energy from the Ne by integral multiples of 8.2 MeV if they are characterized by the projectile velocity. The peaks in the  $Z = 9$  and 8 energy spectra, e.g., Fig. 1, occur at 8.2 and 17.2 MeV below the elastic peak and could correspond to a one-proton and a two-proton transfer. Again referring to Fig. 1, the peaks are at 10.7 and 20.5 MeV below the elastic peak for the  $Z = 11$  and 12 spectra, respectively. These values are larger than for  $Z = 9$  and 8, but they are consistent with one- and two-proton transfers. However, for  $Z = 12$  the data are not inconsistent with the transfer of two protons and one neutron.

Angular distributions for both quasielastic and deeply inelastic products are shown for charge states  $Z = 6$  (carbon) to  $Z = 24$  (chromium) in Fig. 4. The solid curves in this figure are there to guide the eye. The rapid increase in the cross section for small angles and for products near the projectile is typical of quasielastic reactions. The angular distributions will be discussed further in Sec. III C.

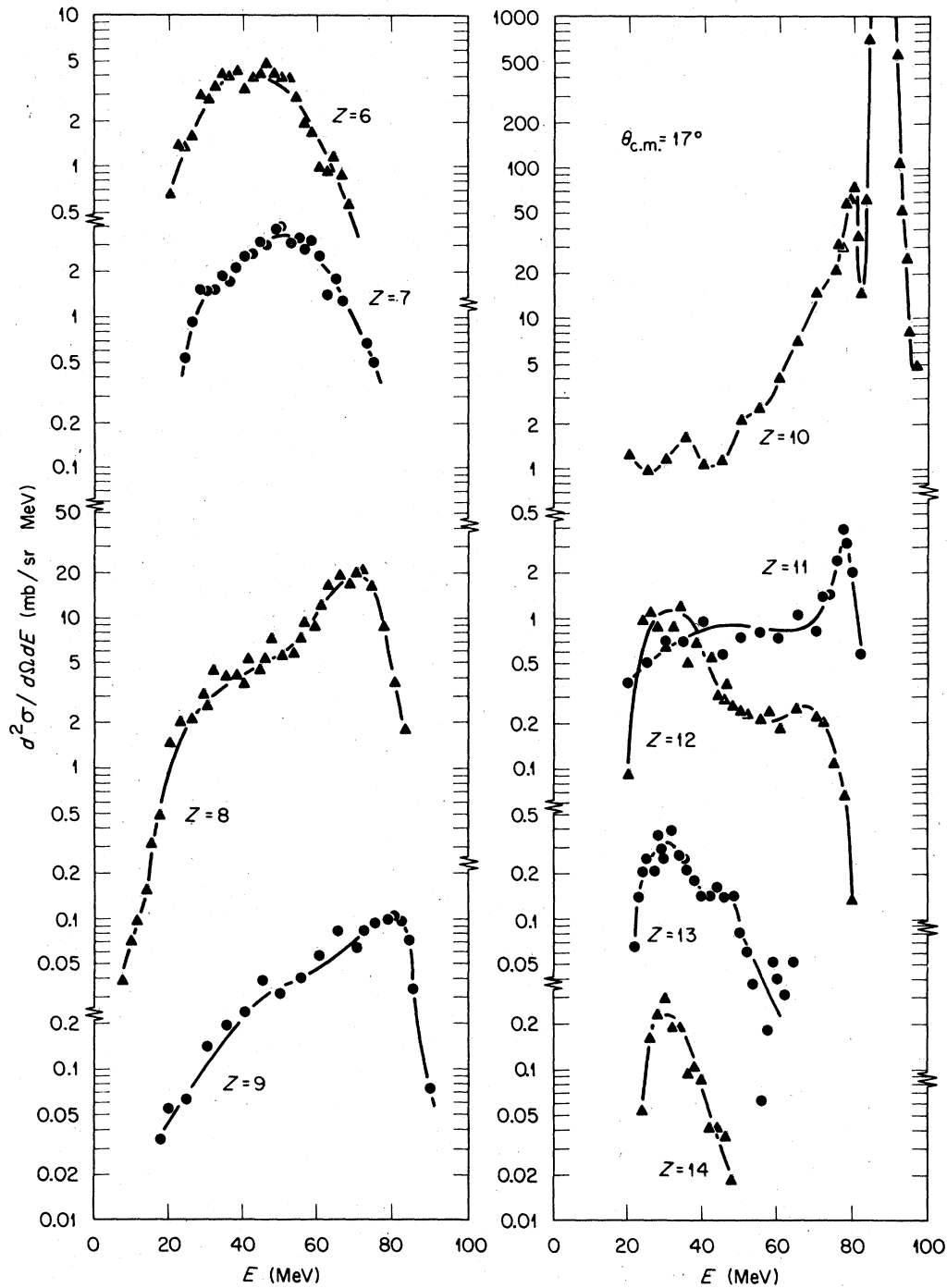


FIG. 1. Center-of-mass energy spectra are shown for  $Z=6$  to  $14$  at a center-of-mass angle of  $17^\circ$ .

### C. Strongly damped reactions

As pointed out above, the deeply inelastic collisions cannot be unambiguously resolved from the quasielastic reactions, and both types of re-

actions appear to belong to the same continuum of processes. Whereas energies of the transfer products are near that of the projectile, the energies of the deeply inelastic products are expected to be near the kinetic energy due to Cou-

lomb repulsion, if complete damping has taken place. The energy spectra Figs. 1-3 show the disappearance of the quasielastic component as the angle is increased. At a center-of-mass angle  $\theta_{c.m.} \gtrsim 35^\circ$  this component appears to be negligible, and all events beyond this angle can be assumed to be strongly damped events. Figure 5 shows the first moment of the energy spectra for  $\theta_{c.m.} = 40^\circ$  as a function of atomic number,  $Z$ .

In order to ascertain the degree of damping in the deeply inelastic events, it is instructive to compare the measured kinetic energies with those expected for fission events. Davies *et al.*<sup>25</sup> have

successfully compared their predictions with a large body of fission kinetic energy data. They predict, for a symmetric mass split ( $Z_1 = Z_2 = 19$ ), that the total-fragment kinetic energy would be 47.4 MeV. This energy, based on deformed spheroids, can be parametrized by two spheres separated by a distance  $S$  such that the total kinetic energy  $E_{TK}$  is given by

$$E_{TK} = \frac{Z^2 e^2}{r_0(2A^{1/3}) + S}, \quad (4)$$

where  $r_0$  is the radius parameter, and  $Z = Z_1 = Z_2$  and  $A = A_1 = A_2$  are the fragment nuclear charges

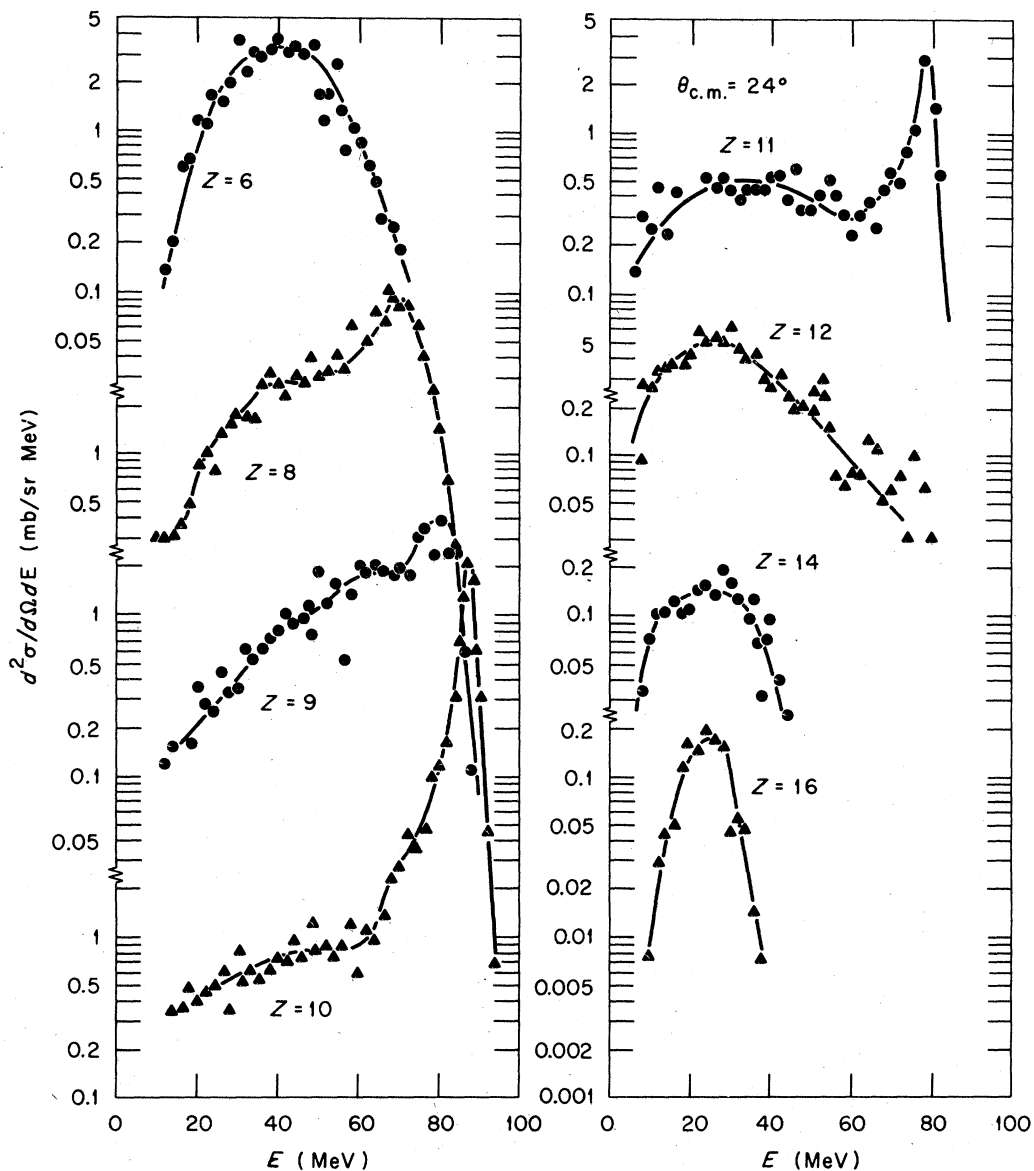


FIG. 2. Center-of-mass energy spectra are shown for  $Z = 6$  to 16 at a center-of-mass angle  $24^\circ$ .

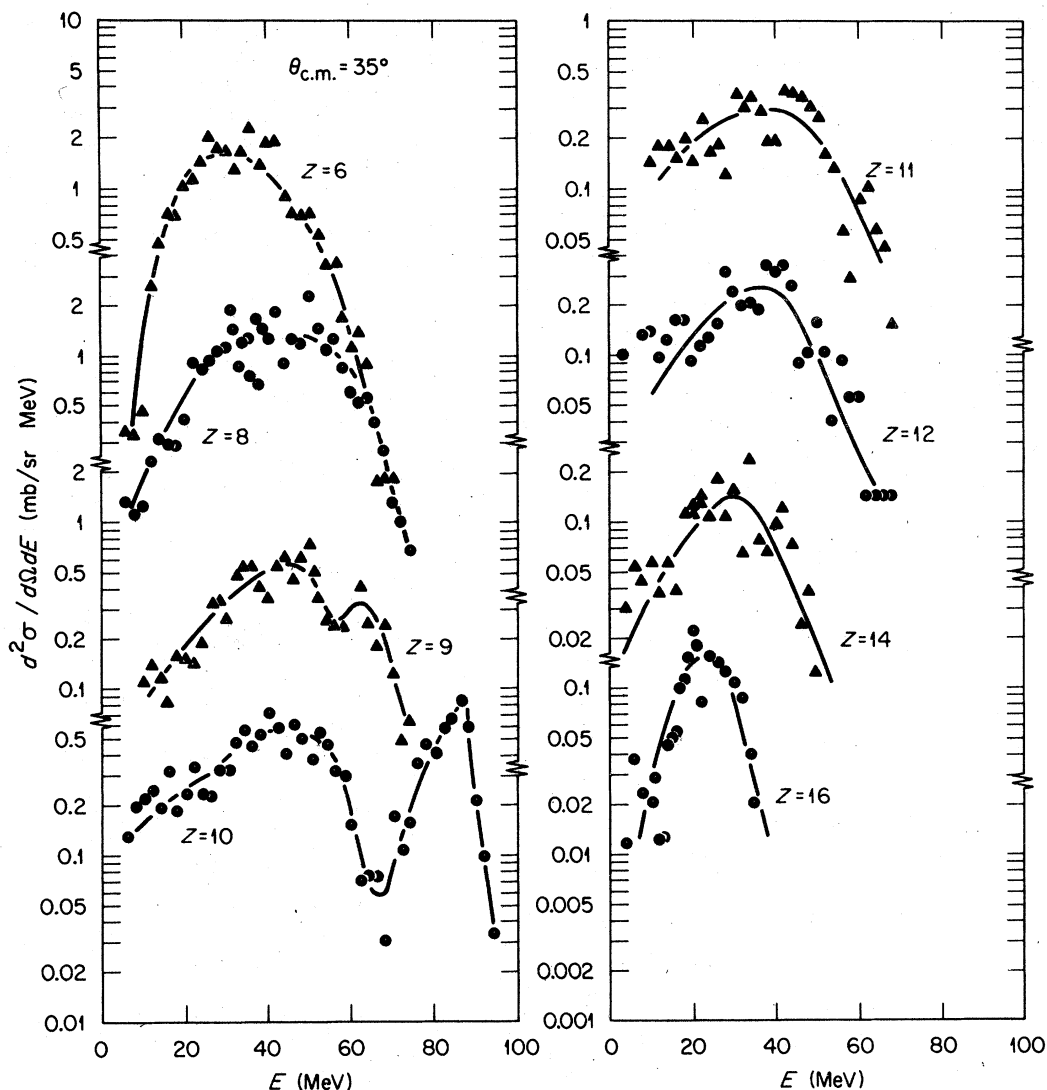


FIG. 3. Center-of-mass energy spectra are shown for  $Z=6$  to  $16$  at a center-of-mass angle  $35^\circ$ . The quasielastic component is no longer observable at this angle.

and masses, respectively. For  $E_{\text{TK}}=47.4$  MeV,  $r_0=1.2$  fm,  $Z=19$ , and  $A=39$ ,  $S$  was found to be  $2.83$  fm. Equation (4) can now be generalized to asymmetric mass splits such that

$$E_{\text{TK}} = \frac{Z_1 Z_2 e^2}{r_0 (A_1^{1/3} + A_2^{1/3}) + S} \quad (5)$$

In this manner, a predicted single-fragment kinetic energy curve (as a function of fragment charge) can be generated. It is indicated in Fig. 5 by the solid curve.

In order to compare the above theoretical prediction directly with the data, we have corrected the calculation for particle emission. If we assume binary events and that a division of available ex-

citation energy is in proportion to the fragment charges, and if effects of angular momentum can be neglected, then the number of particles evaporated from the fragments can be calculated using the statistical model computer code ORNL ALICE.<sup>26</sup> Preevaporation masses and  $Q$  values were used to determine the excitation energy to be shared between the two products. Subsequent particle emission, and thus final products, are determined by calculations that make use of the binding energies of the intermediate nuclei. The change in total kinetic energy due to the mass loss associated with particle emission transforms the solid curve of Fig. 5 to the open circles. It can be seen that there is excellent agreement

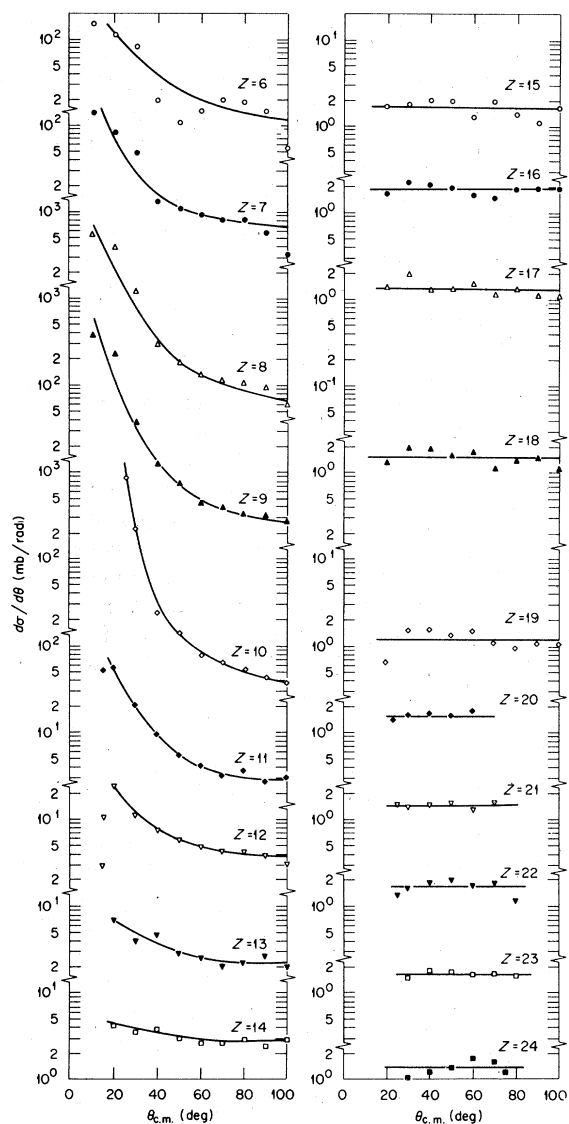


FIG. 4. Center-of-mass angular distributions integrated over particle energy for products  $Z = 6$  to 24. Note that the cross section is  $(d\sigma/d\theta)$ . The flat distributions  $Z > 14$  are indicative of equilibrium processes.

between calculated and experimental points for  $Z \geq 14$ . The higher observed total kinetic energies for  $Z < 14$  are probably due to a combination of two effects. First, for those products relatively close to the projectile, not only has relatively little net mass and charge transfer taken place, but the damping may not be complete. However, this does not imply that such reactions are to be interpreted as direct transfer reactions. Second, it is probable that these light fragments have more nearly spherical shapes than spheroidal shapes, leading to a more compact scission

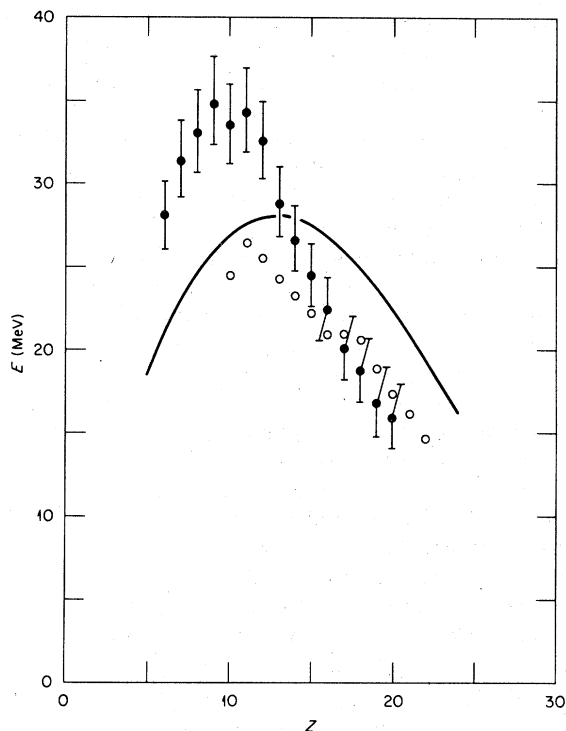


FIG. 5. The energies are single-fragment kinetic energies in the center-of-mass system. The solid curve is theoretical and the open circles are the theoretical results corrected for evaporation.

configuration and hence to higher kinetic energies.

In the above discussion the effects of viscosity and of angular momentum have been neglected. For these very light systems Davies *et al.*<sup>25</sup> have shown that viscosity is not expected to play a role. This is due to the fact that predicted fission barrier shapes are very strongly necked-in, and descent from saddle to scission is very short. For a large body of fission data it has been observed that the fragment total kinetic energies are essentially independent of angular momentum.<sup>17</sup> Eggers *et al.*<sup>14</sup> described large angular momentum effects in the deeply inelastic products from  $^{20}\text{Ne} + ^{27}\text{Al}$ . However, Braun-Munzinger *et al.*<sup>15</sup> have pointed out that a large angular momentum contribution is not required in Ref. 14 if a different charge-separation distance is postulated at the time of scission. They also point out that, in order to determine the angular momentum effects on kinetic energies, data at several energies are required. We shall thus content ourselves with pointing out that our results are consistent with what is expected from fission systematics, without the specific inclusion of an angular momentum component.

The rise at forward angles in the angular dis-

tribution of Fig. 4 for charges near that of the projectile is similar to that observed for  $^{40}\text{Ar} + \text{Th}$ ,<sup>1</sup> and very likely implies contributions from negative angles associated with orbiting.<sup>27</sup> The angular distributions per unit angle  $d\sigma/d\theta$  of products with  $Z \geq 15$  are constant in the center-of-mass system. Thus these products are either fission fragments or were formed during interaction times that were longer than the time required for one rotation of the composite system.

The overall product charge distribution is shown in Fig. 6. The maximum in cross section for the charge products near the charge of the projectile may be characteristic of the quasi-elastic processes and of partially damped events which involve little mass and charge transfer. The centroid of the curve is approximately  $Z = 8$  with a width at half maximum of  $\Delta Z \sim 4$ .

One feature of this distribution is the odd-even effect in the cross section. The yields for the even charges are in most cases larger than the adjacent odd- $Z$  yields. Evaporation calculations described earlier show that the nuclei initially formed in a reaction have a very small probability of survival. For atomic numbers greater than  $Z = 16$ , the probability that no particles will be

emitted or that neutron emission only takes place is less than 5% for any given initial  $Z_i$  and  $A_i$ . Most of the final products are obtained after the emission of at least one proton, and the number of protons evaporated can be as many as four or five. For each final charge  $Z_f$ , the fractional contribution from even- or odd- $Z_i$  initial states can be determined. The results show an even-odd correlation for  $Z_f \geq 16$  and an anticorrelation for  $Z_f < 16$ . It is therefore likely that the even-odd effect has its origin both in the formation of the initial nuclides as well as in the evaporation process.

No evidence is seen for change in the overall charge distribution of Fig. 6 which might correspond to a distinct fission component. Thus it is not clear whether the yield near symmetry ( $Z = 19$ ) arises from the tail of the deeply inelastic charge distribution or from the presence of bona fide fission events, i.e., events that are due to the fission of the compound nucleus. In any case, the yield in this region is very low, and thus symmetric fission, if present at all, accounts for a rather small fraction of the total reaction cross section.

#### D. Evaporation residue products

The composite (fused) system of target and projectile must reach a state of equilibrium in all degrees of freedom in order to become a compound nucleus. The nuclear system can deexcite either by particle emission or by fission. Since the fission contribution was found to be small, we shall equate fusion and compound nucleus formation cross sections with evaporation residue cross sections.

The evaporation residue nuclei have a very forward-peaked angular distribution with a width of only a few degrees determined by the recoil due to evaporation of particles and the multiple scattering in the target. The energy of the evaporation residue products will depend on the number and direction of evaporated particles, but their most probable energy will be near the kinetic energy of the center of mass in the laboratory system.

The measurements of the evaporation residue products were obtained at  $1^\circ$  intervals from  $3^\circ$  to  $20^\circ$  in the laboratory system, with an angular resolution of approximately  $0.25^\circ$ . The major factor governing the precision of the measurements at small angles is the very rapid increase in the Rutherford cross section as the angle decreases. For our detector aperture the change in the cross section is about 40% at  $3^\circ$ . However, since the ER angular distribution also changes

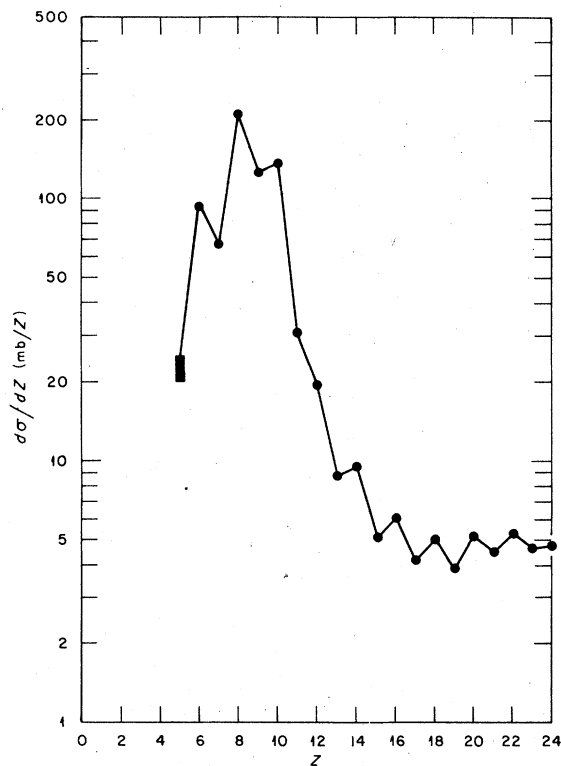


FIG. 6. Cross sections for production of atomic species are shown. Note the odd-even effect in the yield.



rapidly in this region, this uncertainty does not have an appreciable effect on the total ER cross section.

The ER products form a mountain in the  $E'$  versus  $\Delta E$  plane with a ridge running toward  $E' = \Delta E = 0$ . The sum of the events identified as evaporation residues were normalized by the number of elastic events. Since the Rutherford cross section is known, the ER cross section may be calculated from it. The value of the total cross section after integration over angle and energy is  $\sigma_{ER} = (1236 \pm 50)$  mb. This accounts for approximately 61% of the total reaction cross section.

Theoretical calculations of the ER cross section agree quite well with the measured value. The Bass model<sup>28</sup> gives 1270 mb assuming negligible fission, and the evaporation code ALICE<sup>26</sup> gives 1150 mb. Thus the observed fusion cross section is consistent with both the Bass entrance-channel model and with the liquid-drop fission-competition model.<sup>20-22</sup>

#### IV. SUMMARY AND CONCLUSION

The relatively light Ne+Ni system exhibits many features that are similar to those found in reac-

tions between heavier ions and targets. Both quasielastic and deeply inelastic events have been observed. Angular distributions of products with charges near that of the projectile are forward-peaked, indicating the presence of nuclear orbiting similar to that observed in argon-induced reactions. For nuclear charges with  $Z \geq 14$ , the angular distributions per unit solid angle are proportional to  $1/\sin\theta_{c.m.}$ , indicating relatively long reaction times. No sideward peaking was observed. The kinetic energies of products with  $Z \geq 14$  were similar to those predicted by fission theory, implying deformed shapes at the time of scission. The overall charge distribution has even-odd oscillations that could arise both from the intrinsic distribution and from the subsequent deexcitation process. No distinct fission component was identified, but the products from nearly symmetric charge divisions were found to exhibit properties that are consistent with fission characteristics. The evaporation residue cross section is consistent both with an entrance channel description and with a limit imposed by fission competition. The total reaction cross section is well accounted for by the measured reaction products.

\*Department of Chemistry, Tokyo Metropolitan University, Tokyo, Japan.

†Operated by Union Carbide Corporation for the Department of Energy.

<sup>1</sup>A. G. Artukh, G. F. Gridnev, V. L. Mikheev, V. V. Volkov, and J. Wilczynski, Nucl. Phys. **A215**, 91 (1973).

<sup>2</sup>F. Hanappe, M. Lefort, C. Ngô, J. Péter, and B. Taimain, Phys. Rev. Lett. **32**, 738 (1974).

<sup>3</sup>K. L. Wolf, J. P. Unik, J. R. Huizenga, J. Birkelund, H. Freiesleben, and V. E. Viola, Phys. Rev. Lett. **33**, 1105 (1974).

<sup>4</sup>W. U. Schröder and J. R. Huizenga, Annu. Rev. Nucl. Sci. **27**, 465 (1977), and references given therein.

<sup>5</sup>J. Galin, J. Phys. (Paris) **37**, C5-83 (1976), and references therein.

<sup>6</sup>R. Albrecht, W. Dinnweber, G. Graw, H. Ho, S. G. Steadman, and J. P. Wurm, Phys. Rev. Lett. **34**, 1400 (1975).

<sup>7</sup>B. Gatty, D. Guerreau, M. Lefort, X. Tarrago, J. Galin, B. Cauvin, J. Girard, and H. Nifenecker, Nucl. Phys. **A253**, 511 (1975).

<sup>8</sup>J. Barrette, P. Braun-Munzinger, C. K. Gelbke, E. Grosse, H. L. Harney, J. Kuzminski, I. Tserruya, and Th. Walcher, Z. Phys. **A274**, 121 (1975).

<sup>9</sup>P. Braun-Munzinger, C. K. Gelbke, J. Barrette, B. Zeidman, M. J. LeVine, A. Gamp, H. L. Harney, and Th. Walcher, Phys. Rev. Lett. **36**, 849 (1976).

<sup>10</sup>C. K. Gelbke, P. Braun-Munzinger, J. Barrette, B. Zeidman, M. J. LeVine, A. Gamp, H. L. Harney, and Th. Walcher, Nucl. Phys. **A269**, 460 (1976).

<sup>11</sup>J. Barrette, P. Braun-Munzinger, C. K. Gelbke, H. E. Wegner, B. Zeidman, A. Gamp, H. L. Harney, and Th. Walcher, report, 1977 (unpublished).

<sup>12</sup>T. M. Cormier, E. R. Cosman, A. J. Lazzarini, J. D. Garrett, H. E. Wegner, Phys. Rev. C **14**, 127 (1976).

<sup>13</sup>T. M. Cormier, P. Braun-Munzinger, P. M. Cormier, J. W. Harris, and L. L. Lee, Jr., Phys. Rev. C **16**, 215 (1977).

<sup>14</sup>R. Eggers, M. N. Namboodiri, P. Gonthier, K. Geoffroy, and J. B. Natowitz, Phys. Rev. Lett. **37**, 324 (1976).

<sup>15</sup>P. Braun-Munzinger, T. M. Cormier, and C. K. Gelbke, Phys. Rev. Lett. **37**, 1582 (1976).

<sup>16</sup>R. A. Dayras, R. G. Stokstad, M. L. Halbert, D. C. Hensley, C. B. Fulmer, R. Robinson, A. H. Snell, D. G. Sarantites, and L. Westerberg, Report No. ORNL-5306 1977 (unpublished).

<sup>17</sup>F. Plasil, in *Proceedings of the International Conference on Reactions between Complex Nuclei, Nashville, 1974*, edited by R. L. Robinson, F. K. McGowan, J. B. Ball, and J. Hamilton (North-Holland, Amsterdam, 1974), Vol. 2, p. 107, and references therein.

<sup>18</sup>M. L. Halbert, R. G. Stokstad, F. E. Obenshain, F. Plasil, D. C. Hensley, A. H. Snell, R. L. Ferguson, and F. Pleasonton, Report No. ANL/Phys.-76-2, 1976 (unpublished), Vol. 2, p. 601.

<sup>19</sup>R. L. Ferguson, H. Nakahara, F. E. Obenshain, F. Plasil, F. Pleasonton, and A. H. Snell, Bul. Am. Phys. Soc. **22**, 593 (1977); M. P. Webb, F. E. Obenshain, R. L. Ferguson, F. Plasil, F. Pleasonton, and A. H.

- Snell, *ibid.* 22, 593 (1977).
- <sup>20</sup>S. Cohen, F. Plasil, and W. J. Swiatecki, *Ann. Phys.* (N. Y.) 82, 557 (1974).
- <sup>21</sup>M. Blann and F. Plasil, *Phys. Rev. Lett.* 29, 303 (1972).
- <sup>22</sup>F. Plasil and M. Blann, *Phys. Rev. C* 11, 508 (1975).
- <sup>23</sup>R. G. Stokstad, D. C. Hensley, and A. H. Snell, *Nucl. Instrum. Methods* 141, 499 (1977).
- <sup>24</sup>J. S. Blair, *Phys. Rev.* 95, 1218 (1954).
- <sup>25</sup>K. T. R. Davies, A. J. Sierk and J. R. Nix, *Phys. Rev. C* 13, 2385 (1976).
- <sup>26</sup>F. Plasil, Report No. ORNL/TM-6054, 1977 (unpublished).
- <sup>27</sup>J. Wilczynski, *Phys. Lett.* B47, 484 (1973).
- <sup>28</sup>R. Bass, *Nucl. Phys.* A231, 45 (1974).